

An essential role for β -actin mRNA localization and translation in Ca^{2+} -dependent growth cone guidance

Jiaqi Yao¹, Yukio Sasaki², Zhexiong Wen¹, Gary J Bassell² & James Q Zheng¹

Axon pathfinding requires directional responses of growth cones to extracellular cues, which have been shown to involve local synthesis of protein. The identity and functions of the locally produced proteins remain, however, unclear. Here we report that Ca^{2+} -dependent bidirectional turning of *Xenopus laevis* growth cones requires localized distribution and translation of β -actin messenger RNA. Both β -actin mRNA and its zipcode-binding protein, ZBP1, are localized at the growth cone and become asymmetrically distributed upon local exposure to brain-derived neurotrophic factor (BDNF). Inhibition of protein synthesis or antisense interference with β -actin mRNA–ZBP1 binding abolishes both Ca^{2+} -mediated attraction and repulsion. In addition, attraction involves a local increase in β -actin, whereas repulsion is accompanied by a local decrease in β -actin; thus, both produce a synthesis- and ZBP1 binding-dependent β -actin asymmetry but with opposite polarities. Together with a similar asymmetry in Src activity during bidirectional responses, our findings indicate that Ca^{2+} -dependent spatial regulation of β -actin synthesis through Src contributes to the directional motility of growth cones during guidance.

Precise wiring of neuronal circuitry requires developing neurons to extend axonal fibers through a complex environment to seek out their targets for specific connections. Motile growth cones at the tip of elongating axons are responsible for sensing extracellular cues and, subsequently, for steering and growth in specific directions. It is thought that various attractive and repulsive molecules are present in distinct spatiotemporal patterns and work in concert to guide the growth cone to its specific target¹. Growth cones typically react to various guidance molecules with distinct responses, including acceleration of extension, inhibition and/or collapse, and turning toward or away from attractive or repulsive molecules^{1,2}. Although the detailed mechanisms underlying each of these distinct guidance responses are unknown, the cytoskeleton and focal adhesions are thought to be the main targets of intricate guidance signaling. It is conceivable, however, that many other components of growth cone motility are also involved and coordinated to generate distinct guidance responses^{3–5}.

Studies indicate that directional responses of growth cones to guidance cues involve local protein synthesis and degradation^{6–8}; however, the identities of proteins that are locally synthesized and/or degraded at the growth cone and their functions in growth cone motility and pathfinding remain unclear. Recent work indicates that local protein synthesis is involved in regulating guidance receptors on the growth cone surface^{9,10}, but the presence of mRNA molecules encoding signaling and cytoskeletal proteins in the growth cone^{11–14} suggests that membrane receptors may represent only a few of the proteins that are locally synthesized or degraded, or both. Here we first establish that protein synthesis has a downstream role in Ca^{2+} -dependent guidance responses. We then show that asymmetric

localization of β -actin mRNA and its translation at the growth cone are required for Ca^{2+} -dependent growth cone turning. We also present evidence that asymmetric β -actin synthesis is likely to be regulated by asymmetric activity of the Src family of kinases. These findings thus provide important insight into the functional role of spatially regulated β -actin synthesis in Ca^{2+} -dependent bidirectional growth cone steering.

RESULTS

Ca^{2+} -dependent guidance requires local protein synthesis

To assess the role of protein synthesis in guidance, we used cultured embryonic *X. laevis* spinal neurons as a model system and an *in vitro* turning assay for examining growth cone responses to an extracellular gradient of BDNF (Fig. 1). *X. laevis* growth cones from 6-h cultures on glass coverslips coated with poly-D-lysine and laminin were subjected to a BDNF gradient produced through pipette ejection of a BDNF solution^{15–17}. As a control, *X. laevis* growth cones were subjected to pulsatile pipette ejection of a modified Ringer's solution and no effect on the direction of growth cone extension was observed (Fig. 1a). By contrast, *X. laevis* growth cones on the laminin substrate responded to a gradient of BDNF (50 $\mu\text{g ml}^{-1}$ in pipette, $\sim 50 \text{ ng ml}^{-1}$ at the growth cone), with marked attraction toward the BDNF pipette (Fig. 1b). Over a group of 23 neurons examined, a majority of growth cones turned toward the BDNF pipette, resulting in a cumulative distribution of turning angles that shifted to the positive side (Fig. 1d). The average turning angle was $14.3 \pm 4.3^\circ$ (mean \pm s.e.m.) for the BDNF group (Fig. 1e), which was significantly different from the control value ($-0.4 \pm 6.0^\circ$; $P < 0.01$, Mann-Whitney test). By contrast, BDNF-induced

¹Department of Neuroscience and Cell Biology, University of Medicine and Dentistry of New Jersey, Robert Wood Johnson Medical School, 675 Hoes Lane, Piscataway, New Jersey 08854, USA. ²Department of Cell Biology, Emory University School of Medicine, 615 Michael Street, Atlanta, Georgia 30322, USA. Correspondence should be addressed to J.Q.Z. (zhengjq@umdnj.edu).

Received 18 July; accepted 23 August; published online 17 September 2006; doi:10.1038/nn1773



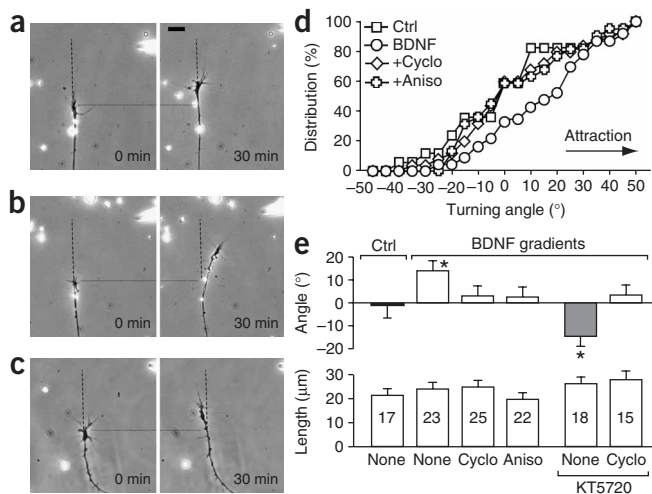


Figure 1 Inhibition of protein synthesis blocks BDNF-induced growth cone turning. (a–c) Representative images of *X. laevis* growth cones showing their responses to pipette application of modified Ringer's solution (a), BDNF solution (b) or BDNF with 25 μM cycloheximide in bath (c). Dotted lines indicate the corresponding positions of the growth cone at the beginning and end of a 30-min turning assay. Dashed lines indicate the original direction of growth cone extension. Scale bar, 20 μm . (d) Cumulative histograms showing the distributions of turning angles from different groups of growth cones exposed to modified Ringer's solution (Ctrl) or a BDNF gradient. Each point indicates the percentage of growth cones bearing a turning angle equal to or less than the value indicated on the x-axis. To inhibit protein synthesis, the indicated inhibitors were added in bath. (e) Average turning angles (top) and lengths of net neurite extension (bottom) of growth cones examined in different groups. Growth cone repulsion induced by BDNF was achieved by inhibiting PKA with 200 nM KT5720 (gray bar). The number of growth cones examined in each group is indicated. Error bars represent the s.e.m. Cyclo, cycloheximide; Aniso, anisomycin. * $P < 0.001$ versus the control (Mann-Whitney test).

attraction was completely abolished in the presence of cycloheximide (25 μM), a ribosomal inhibitor (Fig. 1c). Similarly, BDNF attraction was blocked by bath application of 40 μM anisomycin, another inhibitor of protein synthesis. The blockade of BDNF attraction by these synthesis inhibitors is better depicted by their cumulative distributions of turning angles, which overlapped with that of the control (Fig. 1d). The average turning angles of these two groups also confirmed that no preferential turning was induced by BDNF in the presence of either inhibitor (Fig. 1e).

Previous studies have shown that BDNF-induced growth cone attraction is mediated by Ca^{2+} and can be converted to repulsion by inhibition of protein kinase A (PKA)¹⁶. Accordingly, when PKA was inhibited by 200 nM KT5720 in bath, a gradient of BDNF triggered significant repulsion of *X. laevis* growth cones in culture (Fig. 1e). Bath application of cycloheximide also prevented the repulsive turning (Fig. 1e). Notably, neither of these treatments (protein synthesis inhibition and PKA inhibition) had much influence on the growth cone extension (Fig. 1e). Together, these results show that BDNF-induced bidirectional turning, both attractive and repulsive, requires protein synthesis.

Ca^{2+} is known to mediate BDNF-induced turning responses of growth cones^{16,18}. Is protein synthesis involved downstream or upstream of Ca^{2+} in BDNF-induced turning? To address this question, we examined growth cone turning induced by a direct local increase in intracellular Ca^{2+} concentration ($[\text{Ca}^{2+}]_i$) generated by focal laser-

induced photolysis (FLIP) of caged Ca^{2+} compounds^{19,20} (Fig. 2). Repetitive FLIP of caged Ca^{2+} (NP-EGTA) on one side of the *X. laevis* growth cone induced marked attraction toward the side of focal Ca^{2+} release (Fig. 2a). By contrast, control growth cones without NP-EGTA loading did not show any directional preference in response to repetitive laser exposure (Fig. 2a). Bath application of either cycloheximide or anisomycin eliminated the attraction induced by a local increase in $[\text{Ca}^{2+}]_i$, as assessed by all three cumulative distributions of turning angles (control, cycloheximide and anisomycin), which overlapped and centered at 0° (Fig. 2a). The average turning angles from these groups further showed that inhibition of protein synthesis attenuated the attraction induced by a direct focal increase in $[\text{Ca}^{2+}]_i$ (Fig. 2c).

We also examined the involvement of protein synthesis in growth cone repulsion induced by a direct local increase in $[\text{Ca}^{2+}]_i$. Consistent with previous results^{19,20}, repetitive FLIP on NP-EGTA-loaded growth cones in Ca^{2+} -free bath caused the growth cone to turn away from the FLIP side (repulsion), shifting the cumulative angle distribution to the negative region (Fig. 2b). Similarly, cycloheximide and anisomycin impaired the repulsion, as indicated by their cumulative angle distributions (Fig. 2b) and average turning angles (Fig. 2c). The length of growth cone extension, by contrast, was not affected by these treatments (Fig. 2c). These findings indicate that protein synthesis is required for Ca^{2+} -dependent growth cone turning and is probably involved in events downstream of receptor activation and cytosolic Ca^{2+} signals.

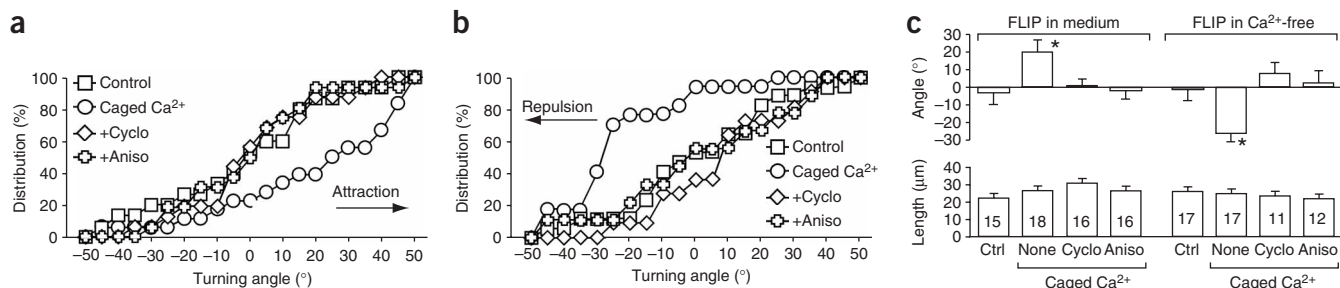


Figure 2 Growth cone turning by FLIP of caged Ca^{2+} depends on protein synthesis. (a) Growth cone attraction induced by repetitive FLIP of caged Ca^{2+} at the growth cone. The cumulative distributions of turning angles show the turning responses under different conditions. (b) Growth cone repulsion induced by FLIP of caged Ca^{2+} in a Ca^{2+} -free solution, as shown by the cumulative distributions of turning angles. (c) Average turning angles and lengths of extension of all growth cones examined under different conditions. Cyclo, cycloheximide; Aniso, anisomycin; Ctrl, control. The number of growth cones examined in each group is indicated. Error bars represent the s.e.m. * $P < 0.001$ versus the control (Mann-Whitney test).

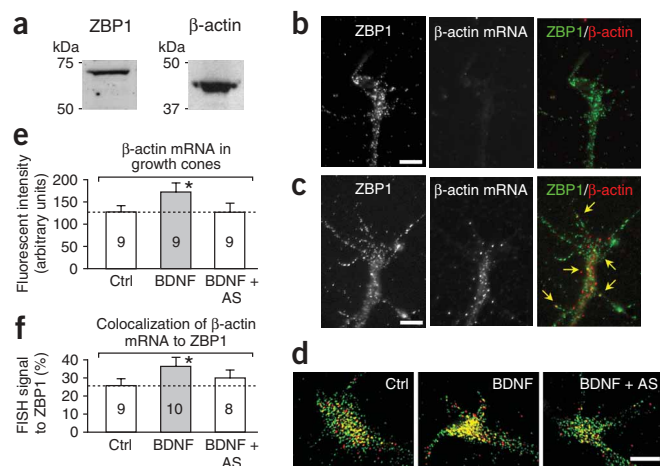


Figure 3 Spatial distribution of β -actin mRNA and ZBP1 proteins in *X. laevis* neurons and growth cones. **(a)** Western blots showing expression of β -actin and ZBP1 in *X. laevis* neural tube tissues. **(b, c)** Spatial distribution of ZBP1 and β -actin mRNA in *X. laevis* growth cones, as detected by fluorescence immunostaining (left) and FISH (middle) with a reverse **(b)** or antisense **(c)** probe. Right images are merged from two channels (green, ZBP1; red, β -actin mRNA); colocalized signals appear in yellow-orange (arrows). Scale bars, 10 μ m. **(d)** Representative images of *X. laevis* growth cones showing the distribution of ZBP1 (green) and β -actin mRNA (red), and their colocalization (yellow) under control (Ctrl), BDNF and BDNF plus antisense (AS) treatments. Scale bar, 10 μ m. **(e)** Average intensities of β -actin mRNA FISH signals in growth cones under the same treatments as in **d**. **(f)** Percentage of β -actin mRNA colocalized to ZBP1 signals in growth cones under the same treatments as in **d**. The number of growth cones examined in each group is indicated. * $P < 0.05$ versus the control (Student's t -test). Error bars represent the s.e.m.

Localization of β -actin mRNA in *X. laevis* growth cones

Studies in chicken forebrain neurons have shown that β -actin mRNA is transported to the growth cone in response to neurotrophin application and that the zipcode-binding protein ZBP1 mediates the translocation of β -actin mRNA²¹. Three ZBP1 homologs, termed VICKZ proteins, are expressed in the developing tissues of many species and function in RNA regulation²². In *X. laevis*, Vg1RBP, a member of this VICKZ family, is involved in localization of Vg1 RNA in oocytes and in migration of neural tube and crest cells²³. The role of these VICKZ proteins in β -actin mRNA localization in *X. laevis* neurons, however, has not been studied. We therefore examined the expression of ZBP1 and β -actin in *X. laevis* spinal neurons (**Fig. 3**).

We used western blotting to analyze purified *X. laevis* neural tubes of embryos at stages 20–22 and detected a β -actin band of 42 kDa and a ZBP1 band of 65–70 kDa with a polyclonal antibody²⁴ (**Fig. 3a**). To examine the distribution of ZBP1 and β -actin mRNA in *X. laevis* growth cones, we carried out immunostaining with a rabbit antibody to ZBP1 (refs. 21,24) and fluorescence *in situ* hybridization (FISH) with digoxigenin-labeled antisense probes for β -actin mRNA²¹. Both β -actin mRNA and ZBP1 were detected in *X. laevis* neurons and appeared as puncta throughout the growth cone, including the filopodia and the axonal shaft (**Fig. 3c**). By contrast, FISH with the reverse probes did not show appreciable signals in these *X. laevis* neurons (**Fig. 3b**). Overall, there appeared to be more ZBP1 puncta than β -actin mRNA puncta in the growth cone. In unstimulated *X. laevis* neurons, only a few β -actin mRNA puncta (10–30%) were colocalized with ZBP1 signals (**Fig. 3c**).

Colocalization analysis was carried out on *X. laevis* growth cones without and with exposure to bath BDNF. The number of colocalized β -actin mRNA and ZBP1 puncta was small in the control growth cone, but it increased markedly upon bath BDNF treatment (200 ng ml⁻¹, 15 min; **Fig. 3d**). To determine whether this increase in colocalized β -actin mRNA–ZBP1 in the growth cone depended on β -actin mRNA binding by ZBP1, we generated three antisense oligonucleotides to *X. laevis* β -actin 3' untranslated region (UTR) zipcodes to block the formation of mRNA–protein complexes²¹ (**Supplementary Fig. 1** online). To create control oligonucleotides, each of these sequences was synthesized in the reversed 5'→3' orientation. Application of all three antisense oligonucleotides (1 μ M each) largely attenuated the BDNF-induced increase in colocalized β -actin mRNA–ZBP1 puncta in the growth cone (**Fig. 3d**). To quantify BDNF effects on the localization of β -actin mRNA and ZBP1 to the growth cone, we first measured the average intensity of FISH signals of β -actin

mRNA and found that bath application of BDNF significantly ($P < 0.05$, Student's t -test) increased β -actin mRNA in the growth cone (**Fig. 3e**). This increase was largely attenuated by the antisense oligonucleotides (**Fig. 3e**). We then quantified the colocalization of β -actin mRNA and ZBP1 in the growth cone. The percentage of β -actin mRNA puncta that colocalized with ZBP1 was significantly increased by BDNF, and this increase was again largely attenuated by the antisense oligonucleotides (**Fig. 3f**). The BDNF-induced increase in β -actin mRNA and ZBP1 colocalization was more apparent in the filopodia (**Supplementary Fig. 2** online). Together, these data indicate that BDNF facilitates localization of β -actin mRNA to the growth cone through ZBP1 binding.

We next investigated whether the distribution of both ZBP1 and β -actin mRNA in the growth cone can be regulated by localized BDNF signals (**Fig. 4**). We found that growth cones exposed to local BDNF application (5 min) showed a local increase in both β -actin mRNA and ZBP1 puncta on the near side of the growth cone to the BDNF pipette (**Fig. 4b**). Notably, the overlapping β -actin mRNA and ZBP1 puncta

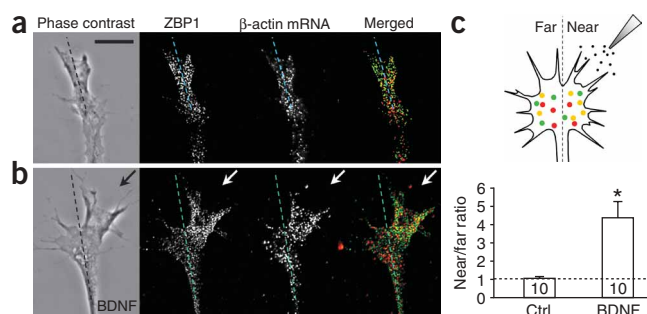


Figure 4 Asymmetric distribution of β -actin mRNA and ZBP1 in growth cones during response to local BDNF application. **(a, b)** Representative images of a control growth cone **(a)** and a growth cone subjected to local BDNF application through a micropipette **(b)**. From left to right, the images show morphology (phase contrast), ZBP1 distribution (immunostaining), β -actin mRNA (FISH) and colocalization (yellow-orange) of ZBP1 (green) and β -actin mRNA (red). Arrows indicate the BDNF gradient. Dashed lines indicate the original direction of growth cone extension. Scale bar, 10 μ m. **(c)** Quantification of the asymmetry of colocalized particles (yellow) between β -actin mRNA (red) and ZBP1 (green) in the growth cone. To evaluate the asymmetry, a near/far ratio was calculated by dividing the number of colocalized β -actin mRNA–ZBP1 particles on the near side by that on the far side. Bar graph shows the near/far ratios of colocalized β -actin mRNA–ZBP1 particles in control (Ctrl) growth cones and growth cones subjected to local BDNF exposure. The number of growth cones examined in each group is indicated. * $P < 0.01$ versus the control (Student's t -test).

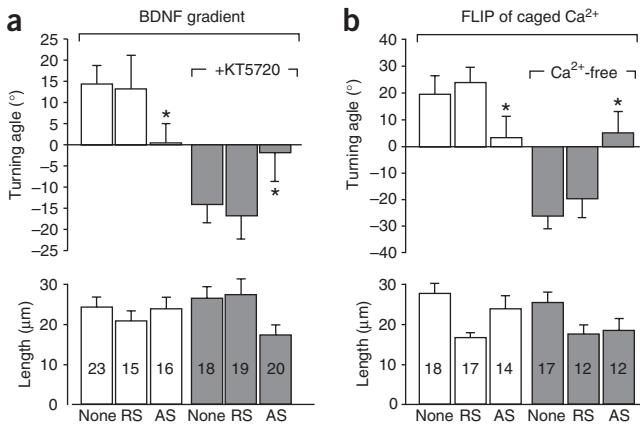


Figure 5 Ca²⁺-dependent growth cone turning depends on β -actin mRNA–ZBP1 interactions. **(a)** Growth cone turning induced by BDNF gradients in the presence of antisense (AS) and control (RS) oligonucleotides. Average angles (top) and lengths (bottom) were derived from all growth cones examined in each group. The number of growth cones examined for each group is indicated. BDNF-induced repulsion was achieved by inhibition of PKA through bath application of KT5720 (200 nM). Repulsion is represented by negative angles in gray bars. **(b)** Growth cone turning induced by repetitive FLIP of caged Ca²⁺. Growth cone repulsion was induced by repetitive FLIP of caged Ca²⁺ when cells were placed in a Ca²⁺-free solution. Asterisks indicate significant difference from the group without any oligonucleotide in bath (None; $P < 0.01$, Mann-Whitney test). Error bars represent the s.e.m.

appeared to be preferentially distributed to the BDNF side of the growth cone (Fig. 4b). By contrast, growth cones without BDNF exposure showed a uniform distribution of β -actin mRNA and ZBP1 throughout the growth cone (Fig. 4a). We quantified the colocalized β -actin mRNA–ZBP1 puncta on the two sides of the growth cone and calculated the near/far ratio (Fig. 4c). Local BDNF application was found to increase significantly ($P < 0.01$, Student's *t*-test) the near/far ratio of colocalized β -actin mRNA and ZBP1 (ratio ≈ 4), whereas the control growth cones showed a symmetric distribution of colocalized β -actin mRNA and ZBP1 (ratio = 1). These observations indicate that local BDNF can induce the preferential distribution of β -actin mRNA–ZBP1 to the side of the growth cone exposed to higher BDNF concentrations. It is conceivable that dynamic translocation of β -actin mRNA by ZBP1 may represent an important step in the directional responses of growth cones to BDNF gradients.

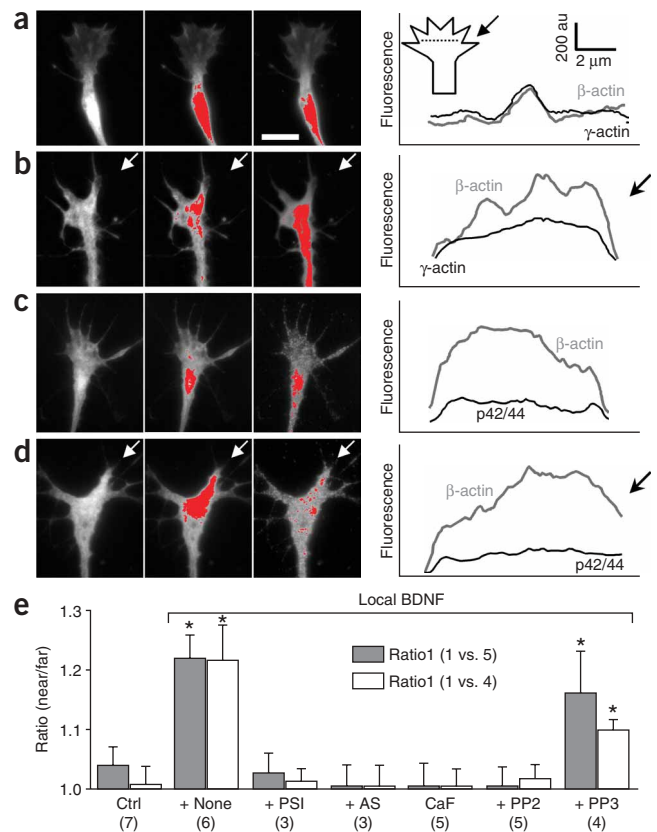
Turning responses require β -actin mRNA–ZBP1 interactions

To determine whether β -actin mRNA binding by ZBP1 is involved in growth cone guidance, we used the antisense oligonucleotides to interfere with binding of β -actin mRNA to ZBP1. For effective blockade of β -actin mRNA–ZBP1 interactions without adversely affecting growth cone motility, all three antisense oligonucleotides were used but at a low concentration (1 μ M each). Whereas the control

oligonucleotides (1 μ M each) had no effects on BDNF-induced attraction, the antisense oligonucleotides abrogated the attraction (Fig. 5a). We also examined BDNF-induced growth cone repulsion in the presence of the PKA inhibitor KT5720. Addition of the antisense oligonucleotides eliminated the repulsion, whereas the control oligonucleotides did not (Fig. 5a). The effects of antisense oligonucleotides on growth cone turning did not seem to result from nonspecific impairment of the ability of the growth cone to move and turn: growth cones subjected to the low concentrations of antisense oligonucleotides still showed substantial extension and random turning, without directional preference.

We also used the antisense approach to further evaluate the role of β -actin mRNA–ZBP1 interactions in growth cone turning induced by a direct focal increase in $[Ca^{2+}]_i$. The control oligonucleotides did not affect growth cone attraction or repulsion induced by repetitive FLIP of caged Ca²⁺ (Fig. 5b). By contrast, addition of the antisense oligonucleotides blocked Ca²⁺-induced attraction and repulsion (Fig. 5b). Together, these results show that interactions between

Figure 6 Asymmetric increase in β -actin in growth cones by local BDNF application. **(a,b)** Representative images showing double immunostaining of β -actin and γ -actin in *X. laevis* growth cones with **(b)** and without **(a)** local BDNF application. Left, for each growth cone, the first two images show β -actin staining and the third shows γ -actin. To visualize the asymmetry, a threshold of 70% was applied to both β - and γ -actin images, leaving the top 30% of intensities highlighted in red. Right, a horizontal line crossing the growth cone was used to generate line profiles based on the original 16-bit images. The fluorescence intensities for β -actin and γ -actin (background-subtracted) are shown in arbitrary units. Arrows in **b** indicate the BDNF gradient. Scale bar, 10 μ m. **(c,d)** Representative images showing double immunostaining of β -actin and p42/44 in *X. laevis* growth cones treated as in **a,b**. **(e)** Quantitative analysis of β -actin asymmetry by the five-box method (Supplementary Fig. 3 online). Bar graph shows the near/far ratios from different groups of growth cones under control (Ctrl) and local BDNF application with different bath treatments (None, nothing added; PSI, protein synthesis inhibitors; AS, antisense oligonucleotides; CaF, Ca²⁺-free; PP2, Src inhibitor; PP3, ineffective Src inhibitor). A ratio of 1 means no asymmetry between the near and far sides; a ratio above 1 indicates more β -actin on the near side than on the far side. The number of growth cones quantified for each group is indicated. * $P < 0.01$ versus the control group (Student's *t*-test). Error bars in **e** represent the s.e.m.



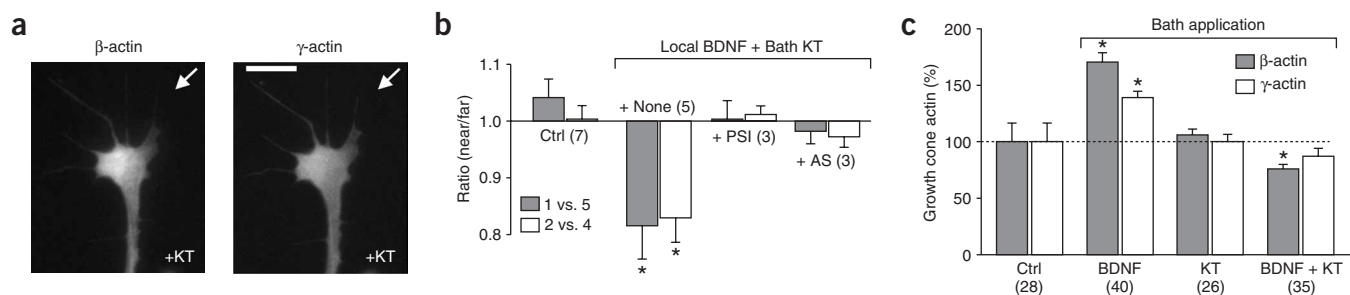


Figure 7 Reverse asymmetry of β -actin distribution in growth cones during repulsion induced by a BDNF gradient under PKA inhibition. **(a)** Representative fluorescence images of β - and γ -actin in a *X. laevis* growth cone exposed to a 5-min local application of BDNF (arrows) under global PKA inhibition by KT5720. Scale bar, 10 μ m. **(b)** Quantitative analysis of β -actin asymmetry by the five-box method. Bar graph shows the near/far ratios from different groups of growth cones under control (Ctrl) and local BDNF application with different bath treatments (None, nothing added; PSI, protein synthesis inhibitors; AS, antisense oligonucleotides). A ratio of 1 indicates no asymmetry; a ratio below 1 indicates more β -actin on the far side than on the near side (reverse asymmetry). The number of growth cones quantified for each group is indicated. * $P < 0.01$ versus the control group (Student's *t*-test). **(c)** Quantification of global β -actin and γ -actin in *X. laevis* growth cones in response to bath application of BDNF, KT5720 or BDNF plus KT5720. Immunostaining of β -actin and γ -actin and subsequent fluorescence imaging were identical for each group (Methods). For all groups, the intensities of β -actin and γ -actin immunofluorescence at the growth cones were normalized to the average of the corresponding control group. As a result, the control group yields a value of 100%. The number of growth cones analyzed for each group is indicated. * $P < 0.02$ versus the control (Student's *t*-test). Error bars represent the s.e.m.

β -actin mRNA and ZBP1 are required for growth cone turning in either an attractive or repulsive direction. Because turning induced by extracellular BDNF gradients and turning induced by direct local increase in $[Ca^{2+}]_i$ were both blocked by antisense oligonucleotides, our findings also indicate that ZBP1-mediated β -actin mRNA translocation probably functions downstream of Ca^{2+} in growth cone steering.

Asymmetric distribution of β -actin in turning responses

Because ZBP1 not only is involved in β -actin mRNA translocation but also regulates β -actin translation²⁵, β -actin mRNA–ZBP1 interactions may give rise to asymmetric synthesis of β -actin proteins at the growth cone for directional steering. We therefore carried out double immunostaining to examine the distribution of β -actin and γ -actin proteins in growth cones exposed to local BDNF (Fig. 6). The specificity of antibodies to β -actin and γ -actin on *X. laevis* neural tube tissues was verified by two-dimensional gel electrophoresis followed by western blotting (data not shown). Simultaneous imaging of both fluorescence channels of the growth cone was done to assess and to compare accurately the spatiotemporal patterns of β -actin and γ -actin in the same growth cone (Methods). Local BDNF application induced an asymmetric increase in β -actin across the growth cone as compared with γ -actin (Fig. 6b). Line intensity profiles of β -actin and γ -actin immunofluorescence showed that BDNF induced a much higher increase in β -actin on the side near the BDNF pipette (Fig. 6b). The slight local increase in γ -actin might be attributed to copolymerization of the β - and γ -actin proteins. Growth cones that were not exposed to BDNF gradients showed similar and even distributions of both β -actin and γ -actin immunofluorescence (Fig. 6a). Double immunostaining of β -actin and p42/44 was also done to verify the β -actin asymmetry induced by BDNF gradients. Consistent with this, a gradient of BDNF induced a similar asymmetry in β -actin but not in p42/44 (Fig. 6d), whereas the control growth cone showed a symmetric distribution of both β -actin and p42/44 (Fig. 6c).

To quantify the β -actin asymmetry, we placed five boxes of equal size across the growth cone, measured the fluorescence intensities of both β -actin and γ -actin within these boxes, and then calculated two near/far β -actin ratios normalized to the corresponding γ -actin ratios (Supplementary Fig. 3 and Supplementary Methods online). Control growth cones showed no asymmetry: both ratios were close to 1 (Fig. 6e).

Local BDNF application increased the ratios to about 1.2, however, indicating that more β -actin was detected on the side near the BDNF pipette (Fig. 6e). A similar asymmetry was also observed when the β -actin ratios were normalized to those of p42/44 (Supplementary Fig. 3 online). This asymmetry in β -actin depended on protein synthesis and was blocked by the protein synthesis inhibitors (Fig. 6e). In addition, when the antisense oligonucleotides were applied, the BDNF-induced asymmetric increase in β -actin was abolished (Fig. 6e). Removal of extracellular Ca^{2+} or inhibition of the Src family of kinases by the pharmacological inhibitor PP2, but not the ineffective PP3, also diminished the asymmetry in β -actin distribution (Fig. 6e). These results indicate that BDNF-induced growth cone attraction involves an asymmetric increase in β -actin across the growth cone, and this asymmetry probably involves ZBP1-dependent translocation and translation of β -actin mRNA in a Ca^{2+} - and Src-dependent manner.

Does growth cone repulsion also involve an asymmetry in β -actin distribution? Immunofluorescence imaging showed that the growth cone also produced an asymmetric distribution of β -actin in response to the BDNF gradient in the presence of KT5720. This asymmetry was in a reversed orientation, however, with more β -actin observed on the far side of the growth cone (Fig. 7a; hereafter referred to as 'reverse asymmetry'). Quantitative measurements and analysis by the five-box method showed that the near/far ratios were significantly ($P < 0.02$, Student's *t*-test) below the control value of 1, confirming the existence of reverse asymmetry. This reverse asymmetry in β -actin was eliminated by both the antisense oligonucleotides and the protein synthesis inhibitors (Fig. 7b). Similarly, reverse asymmetry in β -actin was also observed when the data were normalized to p42/44 (Supplementary Fig. 3 online). This reverse asymmetry aligns with the direction of growth cone repulsion, thus suggesting that the growth cone preferentially steers to the side with more β -actin.

The reverse asymmetry in β -actin during repulsion could be generated by two possible mechanisms: a decrease in β -actin on the near side or an increase in β -actin on the far side. To explore these mechanisms, we used quantitative immunofluorescence imaging to determine the amounts of β - and γ -actin proteins in growth cones exposed to global application of BDNF and BDNF plus KT5720. All groups of cells were processed for immunostaining and imaged identically, and the fluorescence intensities were normalized against

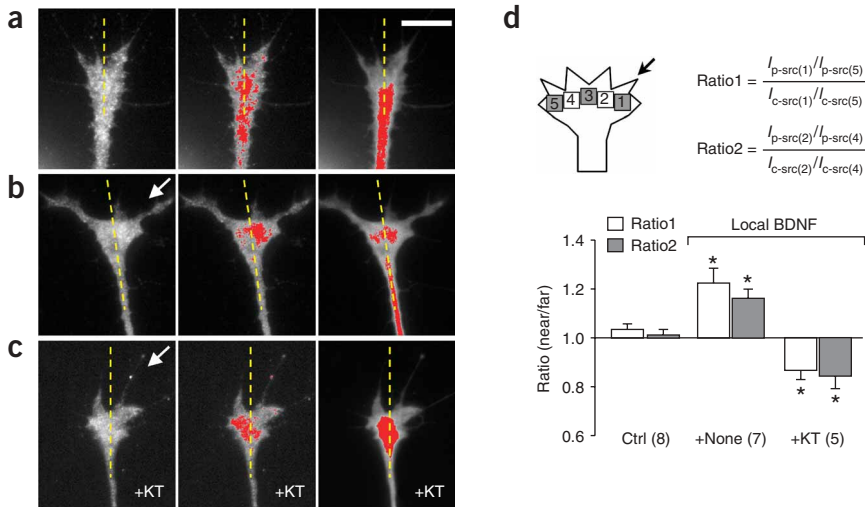


Figure 8 Asymmetric activation of the Src family of kinases by BDNF gradients. (a–c) Representative images showing the spatial patterns of phospho-Src (p-src) and total Src (c-src) staining in growth cones exposed to the control (a), a BDNF gradient (b) and a BDNF gradient plus KT5720 (c). For each condition, the first two images show p-src staining and the third shows c-src staining. To visualize the asymmetry in spatial distribution, a threshold of 70% was applied to both p-src and c-src images, leaving the top 30% of intensities highlighted in red. Scale bar, 10 μm . Arrows indicate the BDNF gradient. (d) Quantitative analysis of asymmetry in p-Src staining by the five-box method. Ctrl, control. All intensity measurements were taken from the original 16-bit images and background-corrected. The equations state the calculation method used to generate two near/far ratios. * $P < 0.02$ versus the control (Student's *t*-test). The number of growth cones examined for each condition is indicated. Error bars represent the s.e.m.

the corresponding control average (Methods). We found that bath application of BDNF for 15 min (200 ng ml⁻¹) resulted in a significant increase in β -actin at the growth cone (Fig. 7c), whereas γ -actin seemed to be affected only modestly. By contrast, 15-min bath application of BDNF to cells pretreated with KT5720 resulted in a reduction in β -actin at the growth cone without affecting γ -actin (Fig. 7c). KT5720 treatment alone did not change the amounts of either β -actin or γ -actin at the growth cone. None of these short-term bath treatments seemed to affect the morphology and motility of *X. laevis* growth cones significantly, but whether long-term manipulations of PKA activity, together with BDNF application, affect growth cones remains to be determined. Nevertheless, these observations, together with the observed opposite β -actin asymmetries, suggest that the BDNF gradient induces a local increase in β -actin on the near side of the growth cone during attraction, but decreases β -actin translation locally on the near side when PKA is inhibited. In the latter case, the local decrease in β -actin translation could generate a reverse asymmetry for repulsion.

Asymmetric Src activation during bidirectional responses

Studies have shown that β -actin translation is regulated by Src-dependent phosphorylation of ZBP1 (ref. 25). Because Ca²⁺-dependent growth cone turning (both attraction and repulsion) also requires Src activities (data not shown) and BDNF is known to regulate Src activities²⁶, we considered that BDNF gradients might induce asymmetric phosphorylation of Src kinases to regulate β -actin translation, thereby creating a specific pattern of β -actin asymmetry for distinct turning responses. Such a hypothesis was partially supported by our imaging data showing that Src inhibition attenuated the β -actin asymmetry induced by the BDNF gradient (Fig. 6e). We therefore used double immunostaining to examine the spatial distribution of phosphorylated Src (phospho-Src) and total Src proteins in growth cones undergoing attraction and repulsion induced by BDNF (Fig. 8). We found that BDNF gradients alone (causing attraction) induced an asymmetry of phospho-Src, with more on the near side of the growth cone (Fig. 8b). In the presence of KT5720, however, local BDNF induced a reverse asymmetry of phospho-Src, with more phospho-Src observed on the far side (Fig. 8c). In both cases, the staining for total Src did not show any asymmetry. Accordingly, control growth cones showed an even distribution of phospho-Src across the growth cone.

Similar to our analysis of β -actin asymmetry, we used the five-box method to determine the distribution of phospho-Src and calculated the near/far ratios (Fig. 8d). In support of our hypothesis, BDNF gradients alone induced a local increase in phospho-Src on the near side of the growth cone, whereas KT5720 inhibition of PKA reversed the asymmetry induced by BDNF (Fig. 8d). Together with the imaging data on the β -actin asymmetry, our data support a model in which BDNF gradients spatially regulate the synthesis of β -actin at the growth cone through Ca²⁺ and Src to create an asymmetry that aligns with the direction of growth cone steering (Supplementary Fig. 4 online).

DISCUSSION

Increasing evidence indicates that local protein synthesis has an important role in growth cone pathfinding during development and regeneration, but the identities of the specific proteins that are synthesized in the growth cone remain unknown^{9,10,13,27–30}. It is also unclear which cellular events during growth cone guidance require new protein production. Here we have used unique turning assays involving extracellular guidance gradients and a direct increase in [Ca²⁺]_i to examine the role of protein synthesis in Ca²⁺-dependent growth cone guidance, and have obtained three main findings. First, protein synthesis is involved in downstream of receptor activation and Ca²⁺ signaling during turning responses. Second, ZBP1-mediated localization of β -actin mRNA and its translation are essential for bidirectional turning. Third, guidance gradients induce an asymmetric distribution of β -actin by increasing or decreasing local β -actin synthesis through Src kinases to create an asymmetry of opposite orientations for attraction or repulsion, respectively. These findings highlight the importance of spatially regulated synthesis of cytoskeletal proteins in directional control of growth cone steering during axon guidance.

Among the many mRNA molecules in the growth cone, β -actin mRNA is actively transported to the growth cone through the zipcode-binding protein ZBP1 (refs. 21,31). Notably, translocation of β -actin mRNA can be regulated by neurotrophin signaling^{21,32}. In our study, BDNF gradients induced asymmetric distribution of β -actin mRNA and ZBP1, consistent with the increase in β -actin mRNA–ZBP1 puncta observed in the growth cone on exposure to bath BDNF. The asymmetry of β -actin mRNA and ZBP1 during growth cone responses to guidance gradients is also supported by live imaging work, in which

the green fluorescent protein (GFP)-tagged ZBP1 homolog Vg1RBP becomes dynamically localized in filopodia on exposure to a netrin-1 gradient³³. Such dynamic localization of β -actin mRNA and ZBP1 or Vg1RBP may underlie the asymmetric production of β -actin in the growth cone for directional steering. Consistently, we found that disruption of β -actin mRNA–ZBP1 binding by antisense oligonucleotides blocked bidirectional turning responses induced by either BDNF gradients or a direct local increase in $[Ca^{2+}]_i$. Previous analyses have shown that delocalization of β -actin mRNA by zipcode antisense oligonucleotides in fibroblasts reduces cell migration and polarization³⁴, and similar antisense oligonucleotides promote retractive behaviors of chicken forebrain growth cones²¹. The blockade of attraction and repulsion observed here, however, is unlikely to result from the effects of our antisense oligonucleotides on basal motility. The antisense oligonucleotides were developed specifically for the zipcode sequences of *X. laevis* β -actin mRNA and used at a low concentration. *X. laevis* growth cones exposed to the antisense oligonucleotides extended substantially and turned in random directions, and application of a single antisense oligonucleotide did not block the turning responses (data not shown), indicating that these oligonucleotides are unlikely to have nonspecific effects. Because ZBP1 is associated with the cytoskeleton and can translocate on either microtubules or microfilaments³⁵, we speculate that Ca^{2+} -dependent reorganization of the cytoskeleton might influence the docking of β -actin mRNA–ZBP1 ribonucleoproteins on the near side of the growth cone as a means to bias directional steering further through local β -actin synthesis.

In addition to β -actin mRNA transport, ZBP1 regulates spatial β -actin translation in a zipcode-dependent manner²⁵. Localization of β -actin mRNA and its regulated translation by ZBP1 could provide a crucial mechanism for the asymmetric synthesis of β -actin in the growth cone responsible for directional steering. Indeed, we show that BDNF gradients induce an asymmetrical increase in β -actin proteins during attractive responses but a reverse β -actin asymmetry during repulsion (in the presence of PKA inhibition). Notably, both patterns of β -actin asymmetry depend on protein synthesis and β -actin mRNA–ZBP1 binding. Given that inhibition of protein synthesis or antisense interference of β -actin–ZBP1 binding completely blocked attraction and repulsion, these results support the notion that ZBP1-mediated asymmetric translation of β -actin is required for bidirectional turning of the growth cone.

How does the BDNF gradient produce β -actin asymmetry with opposite orientations under attraction and repulsion settings? BDNF is known to act through Ca^{2+} to induce growth cone turning^{16,18}, and different sizes of local Ca^{2+} signals can mediate bidirectional turning responses^{19,20,36,37}. Local Ca^{2+} signals are thought to act on the balance of phosphorylation and dephosphorylation of downstream targets to direct the steering^{20,38}. Because Src-dependent phosphorylation of ZBP1 regulates β -actin translation²⁵ and Ca^{2+} -dependent bidirectional turning depends on Src activity (data not shown), a local increase or decrease in β -actin during attraction or repulsion could be induced by local activation or inhibition of Src kinases. In support of this hypothesis, BDNF gradients induced an asymmetric increase in phosphorylation of Src, with more on the near side of the growth cone. By contrast, PKA inhibition resulted in a reversal of this BDNF-induced asymmetry of phospho-Src.

In our current model (Supplementary Fig. 4 online), BDNF-induced growth cone attraction involves local activation of Src to elicit local β -actin translation (on the near side), whereas repulsion (under PKA inhibition) involves local inhibition of Src to decrease β -actin translation (on the near side). In both cases, an asymmetry in Src phosphorylation and β -actin translation is generated (but in

opposite orientations) that may underlie attraction and repulsion, respectively. Studies have shown that phosphorylation of ZBP1 by Src leads to loss of translational repression by decreasing the binding of ZBP1 to β -actin mRNA, thereby facilitating local synthesis at the membrane²⁵. We speculate that, during attractive turning responses, Src activation on the near side of the growth cone may lead to docking and phosphorylation of ZBP1 at sites of activated Src, where activation of β -actin mRNA translation may occur. During repulsive turning responses, local inhibition of Src may lead to decreased phosphorylation of ZBP1 on the near side, favoring translational repression. A prediction of this model is that there may be asymmetric regulation in the localization of phosphorylated ZBP1 across the growth cone. Future studies are required to validate this prediction and to evaluate this model further.

Both the β - and γ -isoforms of actin are expressed in the nervous system, but the β -isoform seems to be preferred for rearrangement of the actin cytoskeleton during signal transduction^{31,39}. The unique amino terminus of β -actin may facilitate its polymerization at submembranous sites, where local synthesis can lead to focal accumulation of nucleation sites⁴⁰. In addition, studies in non-neuronal cells indicate that actin proteins are largely glutathionylated, which limits their polymerization into filaments⁴¹. Local synthesis of new β -actin proteins could provide β -actin molecules, nuclei or both to elicit the local assembly of actin that underlies preferential protrusion of lamellipodia and filopodia during attraction⁴². In agreement with this, filopodia protrusion elicited by a KCl-induced increase in $[Ca^{2+}]_i$ (ref. 43) was blocked by both the protein synthesis inhibitors and the antisense oligonucleotides (Supplementary Fig. 5 online), suggesting that local β -actin synthesis contributes to actin-based filopodia protrusion and growth cone motility. Whereas repulsive turning could be driven by local inhibition of motility through a local decrease in β -actin synthesis owing to Src inhibition. We therefore argue that local regulation of β -actin synthesis could be an important mechanism for triggering directional motility responses of the growth cone to extracellular cues. This model could also explain why global inhibition of protein synthesis or β -actin translation does not impair normal growth cone extension and random turning, which may depend on the existing pool of actin proteins and fluctuations in their spatial dynamics, respectively.

Our findings that asymmetric regulation of β -actin translation underlies directional responses of the growth cone are supported by an independent study³³. Both studies indicate that local β -actin synthesis has a crucial role in growth cone guidance; however, morpholino knockdown of β -actin does not seem to prevent netrin-1-induced growth cone repulsion on a high-concentration laminin substrate³³, indicating some differences between the two studies on repulsion. Although distinct cell types and repulsion conditions may contribute to the apparent discrepancy between these results on repulsion, the specific approaches used for interfering with β -actin translation could be the key. Our antisense oligonucleotides target the zipcode regions to prevent β -actin mRNA–ZBP1 interactions and can thus impair ZBP1 regulation of β -actin translation. As a result, a local decrease in β -actin (presumably mediated by Src–ZBP1) during repulsion would be blocked by our antisense oligonucleotides, but probably not by the morpholino. The finding that protein synthesis inhibitors also removed the reverse asymmetry in repulsion suggests that a baseline level of β -actin translation, together with the local decrease, may underlie the reverse asymmetry for repulsion. Alternatively, local synthesis of other proteins, such as the actin depolymerizing factor ADF/cofilin⁴⁴, could also contribute to the local decrease in β -actin during repulsion. Because ADF/cofilin does not seem to have zipcode

sequences, however, its translation cannot be affected by our antisense oligonucleotides. A definite answer to the repulsion mechanisms awaits further investigation.

Our study has identified β -actin as a key factor in mRNA localization and translation in Ca^{2+} -dependent growth cone guidance. Local synthesis and degradation of other candidate proteins could also contribute to growth cone motility and pathfinding. For example, local translation of RhoA mediates *Sema3A*-induced collapse and is proposed to provide the specificity for *Sema3A* signal transduction⁴⁵, whereas β -actin synthesis is not involved in *Sema3A*-induced repulsion³³. In addition, ADF/cofilin is locally synthesized in the growth cone collapse response to SLIT and *Sema3A* molecules⁴⁴. It is conceivable that local protein synthesis or degradation, or both, may provide specificities to transduce different guidance signals. Future challenges will be to identify those proteins that are locally synthesized and required for growth cone motility and those that are involved in specific signaling. A full understanding of the exact functions of these newly produced proteins would significantly advance our knowledge on growth cone pathfinding during development and provide strategies to enhance axon regeneration and rewiring after injury and disease.

METHODS

***Xenopus laevis* neuronal culture and turning assays.** *X. laevis* neurons grown on poly-D-lysine and laminin were prepared as described⁴⁶ and used 4–6 h after plating. Growth cone turning induced by BDNF gradients or by focal release of caged Ca^{2+} was done as described^{19,20,46} (see **Supplementary Methods** online).

Western blotting. Neural tube tissues were dissociated from *X. laevis* embryos at stages 20–24 and subjected to 1 mg ml⁻¹ of collagenase for 30 min, and then the neural tube was separated from the myotome and notochord tissues⁴⁷. The isolated neural tubes were then homogenized and subjected to a standard blotting procedure with a polyclonal rabbit antibody to ZBP1 (refs. 21,24) and a monoclonal mouse antibody to β -actin (Sigma; see **Supplementary Methods** online).

***In situ* hybridization and immunostaining.** FISH with digoxigenin-labeled probes for β -actin mRNA was done as described^{21,31,32}, followed by immunostaining of ZBP1 with the polyclonal antibody to ZBP1 (see **Supplementary Methods** online). To examine the effects of global BDNF treatment on β -actin mRNA and ZBP1, *X. laevis* neurons were exposed to a bath medium containing 200 ng ml⁻¹ of BDNF, with or without antisense oligonucleotides (1 μM each), for 15 min, then were fixed and analyzed by FISH and immunostaining. To study the distribution of ZBP1 and β -actin mRNA in response to local BDNF, we used our pipette application approach modified so that the pipette was placed 50 μm away from the growth cone at a 45° angle to the original direction of growth cone extension. BDNF (100 μg ml⁻¹) was repetitively pressure-ejected as described for turning (repetitive rate, 2 Hz; pressure, 3 psi; pulse duration, 20 ms). For each culture dish, only one growth cone was subjected to a 5-min local BDNF application, followed by rapid fixation and processing for immunostaining and FISH. Quantitative imaging and analyses of FISH and ZBP1 signals in the growth cones are described in **Supplementary Methods** online.

Quantitative immunofluorescence imaging of β -actin. Quantitative immunofluorescence microscopy was used to examine the global and local effects of BDNF on β - and γ -actin under different conditions. For global effects, *X. laevis* neurons were exposed to a bath medium containing 200 ng ml⁻¹ of BDNF, 500 nM KT5720, or 200 ng ml⁻¹ of BDNF plus 500 nM KT5720 for 15 min, then fixed and immunostained. For experiments involving coapplication of KT5720 and BDNF, the cells were pretreated with KT5720 for 20 min. Each experiment included all four treatment groups and was repeated two or three times using different batches of cultures. To detect asymmetric distribution of β - and γ -actin, or Src-p418 and c-Src, induced by BDNF gradients, one growth cone in each dish was subjected to a 5-min local BDNF application through a

micropipette, followed by rapid fixation and immunostaining. Different inhibitors, antisense oligonucleotides or Ca^{2+} -free buffer were applied to the cells 20 min before the local BDNF application. Detailed experimental procedures for fixation and labeling are provided in **Supplementary Methods** online. To analyze the spatial levels of β -actin, quantitative measurements were made on the original 16-bit images using ImageJ (US National Institutes of Health). Detailed descriptions of the analyses are given in **Supplementary Methods** online.

Note: Supplementary information is available on the Nature Neuroscience website.

ACKNOWLEDGMENTS

We thank C.E. Holt and colleagues (University of Cambridge) for sharing unpublished work and R.H. Singer (Albert Einstein College of Medicine) for the antibody to ZBP1. This work was supported by grants from the US National Institutes of Health (NS36241 to J.Q.Z. and HD46368 to G.J.B.) and a research grant from New Jersey Commission on Spinal Cord Research (04-3029-SCR to J.Q.Z.).

AUTHOR CONTRIBUTIONS

J.Y. performed most of the experiments and analyses in this study. Y.S. designed zipcode antisense and did FISH and immunostaining on β -actin mRNA and ZBP1. Z.W. assisted with the turning assay. G.J.B. contributed to the development of the project and directed the antisense and FISH experiments. J.Q.Z. designed and oversaw the research project, and directed most of the experiments, analyses and writing.

COMPETING INTERESTS STATEMENT

The authors declare that they have no competing financial interests.

Published online at <http://www.nature.com/natureneuroscience>

Reprints and permissions information is available online at <http://npg.nature.com/reprintsandpermissions/>

1. Tessier-Lavigne, M. & Goodman, C.S. The molecular biology of axon guidance. *Science* **274**, 1123–1133 (1996).
2. Dickson, B.J. Molecular mechanisms of axon guidance. *Science* **298**, 1959–1964 (2002).
3. Kalil, K. & Dent, E.W. Touch and go: guidance cues signal to the growth cone cytoskeleton. *Curr. Opin. Neurobiol.* **15**, 521–526 (2005).
4. Dent, E.W. & Gertler, F.B. Cytoskeletal dynamics and transport in growth cone motility and axon guidance. *Neuron* **40**, 209–227 (2003).
5. Korey, C.A. & Van Vactor, D. From the growth cone surface to the cytoskeleton: one journey, many paths. *J. Neurobiol.* **44**, 184–193 (2000).
6. Campbell, D.S. & Holt, C.E. Chemotropic responses of retinal growth cones mediated by rapid local protein synthesis and degradation. *Neuron* **32**, 1013–1026 (2001).
7. Campbell, D.S. & Holt, C.E. Apoptotic pathway and MAPKs differentially regulate chemotropic responses of retinal growth cones. *Neuron* **37**, 939–952 (2003).
8. Ming, G.L. *et al.* Adaptation in the chemotactic guidance of nerve growth cones. *Nature* **417**, 411–418 (2002).
9. Brittis, P.A., Lu, Q. & Flanagan, J.G. Axonal protein synthesis provides a mechanism for localized regulation at an intermediate target. *Cell* **110**, 223–235 (2002).
10. Piper, M., Salih, S., Weinl, C., Holt, C.E. & Harris, W.A. Endocytosis-dependent desensitization and protein synthesis-dependent resensitization in retinal growth cone adaptation. *Nat. Neurosci.* **8**, 179–186 (2005).
11. Moccia, R. *et al.* An unbiased cDNA library prepared from isolated aplysia sensory neuron processes is enriched for cytoskeletal and translational mRNAs. *J. Neurosci.* **23**, 9409–9417 (2003).
12. Willis, D. *et al.* Differential transport and local translation of cytoskeletal, injury-response, and neurodegeneration protein mRNAs in axons. *J. Neurosci.* **25**, 778–791 (2005).
13. Piper, M. & Holt, C. RNA translation in axons. *Annu. Rev. Cell Dev. Biol.* **20**, 505–523 (2004).
14. Lee, S.K. & Hollenbeck, P.J. Organization and translation of mRNA in sympathetic axons. *J. Cell Sci.* **116**, 4467–4478 (2003).
15. Ming, G.L., Lohof, A.M. & Zheng, J.Q. Acute morphogenic and chemotropic effects of neurotrophins on cultured embryonic *Xenopus* spinal neurons. *J. Neurosci.* **17**, 7860–7871 (1997).
16. Song, H.J., Ming, G.L. & Poo, M.M. cAMP-induced switching in turning direction of nerve growth cones. *Nature* **388**, 275–279 (1997).
17. Guirland, C., Suzuki, S., Kojima, M., Lu, B. & Zheng, J.Q. Lipid rafts mediate chemotropic guidance of nerve growth cones. *Neuron* **42**, 51–62 (2004).
18. Li, Y. *et al.* Essential role of TRPC channels in the guidance of nerve growth cones by brain-derived neurotrophic factor. *Nature* **434**, 894–898 (2005).
19. Zheng, J.Q. Turning of nerve growth cones induced by localized increases in intracellular calcium ions. *Nature* **403**, 89–93 (2000).

20. Wen, Z., Guirland, C., Ming, G.L. & Zheng, J.Q.A. CaMKII/calcineurin switch controls the direction of Ca²⁺-dependent growth cone guidance. *Neuron* **43**, 835–846 (2004).
21. Zhang, H.L. *et al.* Neurotrophin-induced transport of a β -actin mRNP complex increases β -actin levels and stimulates growth cone motility. *Neuron* **31**, 261–275 (2001).
22. Yisraeli, J.K. VICKZ proteins: a multi-talented family of regulatory RNA-binding proteins. *Biol. Cell* **97**, 87–96 (2005).
23. Yaniv, K., Fainsod, A., Kalcheim, C. & Yisraeli, J.K. The RNA-binding protein Vg1 RBP is required for cell migration during early neural development. *Development* **130**, 5649–5661 (2003).
24. Farina, K.L., Huttelmaier, S., Musunuru, K., Darnell, R. & Singer, R.H. Two ZBP1 KH domains facilitate β -actin mRNA localization, granule formation, and cytoskeletal attachment. *J. Cell Biol.* **160**, 77–87 (2003).
25. Huttelmaier, S. *et al.* Spatial regulation of β -actin translation by Src-dependent phosphorylation of ZBP1. *Nature* **438**, 512–515 (2005).
26. Robles, E., Woo, S. & Gomez, T.M. Src-dependent tyrosine phosphorylation at the tips of growth cone filopodia promotes extension. *J. Neurosci.* **25**, 7669–7681 (2005).
27. Bassell, G.J. & Kelic, S. Binding proteins for mRNA localization and local translation, and their dysfunction in genetic neurological disease. *Curr. Opin. Neurobiol.* **14**, 574–581 (2004).
28. Steward, O. Translating axon guidance cues. *Cell* **110**, 537–540 (2002).
29. Martin, K.C. Local protein synthesis during axon guidance and synaptic plasticity. *Curr. Opin. Neurobiol.* **14**, 305–310 (2004).
30. Willis, D.E. & Twiss, J.L. The evolving roles of axonally synthesized proteins in regeneration. *Curr. Opin. Neurobiol.* **16**, 111–118 (2006).
31. Bassell, G.J. *et al.* Sorting of β -actin mRNA and protein to neurites and growth cones in culture. *J. Neurosci.* **18**, 251–265 (1998).
32. Zhang, H.L., Singer, R.H. & Bassell, G.J. Neurotrophin regulation of β -actin mRNA and protein localization within growth cones. *J. Cell Biol.* **147**, 59–70 (1999).
33. Leung, K.-M. *et al.* Asymmetrical β -actin mRNA translation in growth cones mediates attractive turning to netrin-1. *Nat. Neurosci.* **9**, 1247–1256 (2006).
34. Kislauskis, E.H., Zhu, X. & Singer, R.H. β -Actin messenger RNA localization and protein synthesis augment cell motility. *J. Cell Biol.* **136**, 1263–1270 (1997).
35. Oleynikov, Y. & Singer, R.H. Real-time visualization of ZBP1 association with β -actin mRNA during transcription and localization. *Curr. Biol.* **13**, 199–207 (2003).
36. Hong, K., Nishiyama, M., Henley, J., Tessier-Lavigne, M. & Poo, M. Calcium signalling in the guidance of nerve growth by netrin-1. *Nature* **403**, 93–98 (2000).
37. Henley, J.R., Huang, K.H., Wang, D. & Poo, M.M. Calcium mediates bidirectional growth cone turning induced by myelin-associated glycoprotein. *Neuron* **44**, 909–916 (2004).
38. Gomez, T.M. & Zheng, J.Q. The molecular basis for calcium-dependent axon pathfinding. *Nat. Rev. Neurosci.* **7**, 115–125 (2006).
39. Shuster, C.B. & Herman, I.M. Indirect association of ezrin with F-actin: isoform specificity and calcium sensitivity. *J. Cell Biol.* **128**, 837–848 (1995).
40. Shestakova, E.A., Singer, R.H. & Condeelis, J. The physiological significance of β -actin mRNA localization in determining cell polarity and directional motility. *Proc. Natl. Acad. Sci. USA* **98**, 7045–7050 (2001).
41. Wang, J. *et al.* Reversible glutathionylation regulates actin polymerization in A431 cells. *J. Biol. Chem.* **276**, 47763–47766 (2001).
42. Zheng, J.Q., Wan, J.J. & Poo, M.M. Essential role of filopodia in chemotropic turning of nerve growth cone induced by a glutamate gradient. *J. Neurosci.* **16**, 1140–1149 (1996).
43. Rehder, V. & Kater, S.B. Regulation of neuronal growth cone filopodia by intracellular calcium. *J. Neurosci.* **12**, 3175–3186 (1992).
44. Piper, M. *et al.* Signaling mechanisms underlying Slit2-induced collapse of *Xenopus* retinal growth cones. *Neuron* **49**, 215–228 (2006).
45. Wu, K.Y. *et al.* Local translation of RhoA regulates growth cone collapse. *Nature* **436**, 1020–1024 (2005).
46. Guirland, C., Buck, K.B., Gibney, J.A., DiCicco-Bloom, E. & Zheng, J.Q. Direct cAMP signaling through G-protein-coupled receptors mediates growth cone attraction induced by pituitary adenylate cyclase-activating polypeptide. *J. Neurosci.* **23**, 2274–2283 (2003).
47. Peng, H.B., Baker, L.P. & Chen, Q. Tissue culture of *Xenopus* neurons and muscle cells as a model for studying synaptic induction. *Methods Cell Biol.* **36**, 511–526 (1991).